

MicroRNA-98-5p regulates the proliferation and apoptosis of A549 cells by targeting MAP4K3

ZIQUAN WANG¹, ZHENGXIANG HAN², LANSHENG ZHANG¹, SHIQIANG ZHANG¹ and BAOQING WANG¹

¹Department of Medical Oncology, General Hospital of Xuzhou Mining Group, The Second Affiliated Hospital of Xuzhou Medical University, Xuzhou, Jiangsu 221006; ²Department of Medical Oncology, The Affiliated Hospital of Xuzhou Medical University, Xuzhou, Jiangsu 221000, P.R. China

Received May 1, 2018; Accepted June 25, 2019

DOI: 10.3892/ol.2019.10771

Abstract. Non-small cell lung cancer (NSCLC) is a primary subtype of lung cancer that is accompanied by a high incidence rate and poor prognosis. The primary treatment for NSCLC is chemotherapy, which has low effectiveness and high toxicity. Thus, novel targeted therapy has drawn much attention in recent years. MicroRNAs (miRs) serve important roles in multiple cancer types. In the current study, a decrease in miR-98-5p and an increase in mitogen-activated protein kinase kinase kinase 3 (MAP4K3) was observed in NSCLC tumor tissues compared with normal tissues. miR-98-5p was predicted to target positions 1,056-1,063 of the MAP4K3 3'-untranslated region (UTR). The binding sites between miR-98-5p and the 3'-UTR of MAP4K3 messenger RNA were supported by the results of a dual-luciferase reporter assay. Compared with the control and miR-negative control (NC) groups, miR-98-5p mimic significantly reduced cell proliferation and increased apoptosis in NSCLC cells. In addition, miR-98-5p mimic reduced the expression of MAP4K3 and mammalian target of rapamycin while increasing the expression of cleaved caspase-3 compared with the control group and miR-NC groups. In conclusion, miR-98-5p may inhibit the progression of NSCLC via targeting of MAP4K3.

Introduction

Globally, lung cancer is the leading cause of cancer-associated mortality (1,2). Non-small cell lung cancer (NSCLC), accounting for ~85% of lung cancer cases, and is primarily divided into two subtypes: Squamous cell carcinoma and adenocarcinoma, which are derived from epithelial cells that

line the larger and peripheral small airways, respectively (3). NSCLC is an aggressive type of cancer that is accompanied by poor overall survival (4). Therefore, investigating the mechanisms of NSCLC progression is of great importance for the development of targeted treatments for this disease.

The mitogen-activated protein kinase kinase kinase (MAP4K) family includes MAP4K1 (5), MAP4K2, MAP4K3 (6), MAP4K4 (7) and MAP4K5, and it is a subtype of the mammalian sterile 20 (Ste20) family (8). Kinases of the MAP4K family are important regulators of MAPK, which modulates multiple cellular functions, including cell proliferation, apoptosis and migration (9,10). MAP4K3 has been previously reported to regulate cell death (11). In hepatocellular carcinoma cell lines, MAP4K3 has also been shown to induce cell migration and invasion (12). Overexpression of MAP4K3 was identified in NSCLC tumor tissues (13), and correlated with recurrence in patients with NSCLC (14).

MicroRNAs (miRs/miRNAs) are a class of small, non-coding RNAs, with a length of 19-24 nucleotides that can reduce the translation or induce the degradation of target messenger RNAs (mRNAs) (15). Specific miRNA expression changes are associated with prognosis in cancer patients (16). miRNAs serve important roles in multiple biological processes, including cell proliferation (17) and apoptosis (18). For the present study, a list of potential miRNAs, including miR-98-5p, that may target MAP4K3 were identified using a bioinformatics approach. A subsequent literature search revealed that miR-98-5p was a member of the let-7 family (19), which has previously been reported to be a regulator of MAP4K3 (13). The current study aimed to explore the potential of this miRNA to regulate MAP4K3 in NSCLC.

Materials and methods

Cell lines and clinical samples. The 293T cells and human NSCLC cell line A549 were purchased from the American Type Culture Collection and cultured in RPMI-1640 medium (Gibco; Thermo Fisher Scientific, Inc.) supplemented with 10% fetal bovine serum (Gibco; Thermo Fisher Scientific, Inc.), 100 U/ml penicillin (Invitrogen; Thermo Fisher Scientific, Inc.) and 100 µg/ml streptomycin (Invitrogen; Thermo Fisher Scientific, Inc.) in an incubator at 37°C with 95% humidified atmosphere and 5% CO₂.

Correspondence to: Dr Baoqing Wang, Department of Medical Oncology, General Hospital of Xuzhou Mining Group, The Second Affiliated Hospital of Xuzhou Medical University, 32 Meijian Road, Xuzhou, Jiangsu 221006, P.R. China
E-mail: wangbaoqingghxz@yeah.net

Key words: non-small cell lung cancer, microRNA-98, cell proliferation, cell apoptosis, MAP4K3

A total of 90 NSCLC specimens and matched adjacent normal tissues were obtained from patients with NSCLC who underwent surgery at the General Hospital of Xuzhou Mining Group, The Second Affiliated Hospital of Xuzhou Medical University (Xuzhou, China) between March 2014 and November 2016. The patients had not received preoperative radiotherapy or chemotherapy. Written informed consent was obtained from each patient or the patient's family. The protocols were approved by the Ethics Committee of the General Hospital of Xuzhou Mining Group.

Cell transfection. miR-98-5p mimic and a negative control (miR-NC) were constructed by Shanghai GenePharm Co., Ltd. A total of 1×10^6 A549 cells/well were seeded in 6-well plates and incubated at 37°C with 5% CO₂ for 24 h to a confluence of 50–60%. Next, A549 cells were transfected with 50 nM miR-98-5p mimic (5'-UGAGGUAGUAAGUUGUAUUGUU-3') or miR-NC (5'-UCGCUUGGUGCAGGUCGGG-3') using Lipofectamine® 2000 (Invitrogen; Thermo Fisher Scientific, Inc.) according to the manufacturer's protocol, and incubated at 37°C for 48 h before the following experiments were performed. Cells were randomly divided into 3 groups: i) Control group, untransfected cells; ii) miR-NC group, cells transfected with miR-NC; and iii) miR-98-5p group, cells transfected with miR-98-5p.

Reverse transcription-quantitative polymerase chain reaction (RT-qPCR). Total RNA was isolated from NSCLC tumor tissues, adjacent normal tissues and NSCLC A549 cells according to the protocol of the miRNeasy Mini kit (Qiagen, Inc.). For detection of mature miRNA, poly(A) tails were added by incubation of RNA (100 ng) with poly(A) polymerase (New England BioLabs, Inc.), followed by RT with oligo-dT adapter primers and Moloney murine leukemia virus (MMLV) polymerase (Invitrogen; Thermo Fisher Scientific, Inc.). For quantification of mRNA, complementary DNAs were synthesized from total RNA using oligo (dT)15 primers and MMLV polymerase (Invitrogen; Thermo Fisher Scientific, Inc.). mRNA and miRNA were reverse-transcribed into cDNA under the following conditions: Incubation at 37°C for 50 min, followed inactivation at 70°C for 15 min. qPCR was performed using SYBR Green PCR Master mix (Toyobo Life Science) on a Light-Cycler 480 Real-Time PCR System (Roche Diagnostics), and the thermocycling conditions were as follows: initial denaturation at 94°C for 2 min, followed by 40 cycles of 94°C for 5 sec and 60°C for 30 sec. The relative levels of miRNA and mRNA were normalized to U6 and GAPDH, respectively. The primer sequences were as follows: MAP4K3 forward, 5'-GACTCCCCTGCAAAAAGTCTG-3' and reverse, 5'-GTCCATAGGTGCCATTTCCAA-3'; GAPDH forward, 5'-TTGGTATCGTGGAAGGACTCA-3' and reverse, 5'-TGTCATCATATTTGGCAGGTT-3'; miR-98-5p forward, 5'-TGAGGTAGTAGTTTGTGCTGTT-3' and reverse, 5'-GCGAGCACAAGTAATACGAC-3'; U6 forward, 5'-TGC GGGTGCTCGCTTCGCAGC-3' and reverse, 5'-CCAGTGCAGGTCCGAGGT-3'. The fold-change in miRNA and mRNA expression was calculated using the $2^{-\Delta\Delta C_q}$ method (20).

Western blotting. Proteins were isolated from NSCLC tumor tissues, adjacent normal tissues and the NSCLC cell line

A549 using radioimmunoprecipitation assay buffer (Roche, Diagnostics) containing a cocktail of complete protease inhibitor (Roche Diagnostics GmbH). Protein samples (20 µg) were separated by SDS-PAGE on an 8–10% gel and blotted onto polyvinylidene difluoride membranes (EMD Millipore). Subsequently, rabbit anti-MAP4K3 antibody (1:1,000 dilution; cat. no. 92427; Cell Signaling Technology, Inc.), rabbit anti-GAPDH antibody (1:5,000 dilution; cat. no. 5174; Cell Signaling Technology, Inc.), rabbit anti-phosphorylated-mammalian target of rapamycin (p-mTOR) antibody (1:1,000 dilution; cat. no. 5536; Cell Signaling Technology, Inc.), rabbit anti-mTOR antibody (1:1,000 dilution; cat. no. 2792; Cell Signaling Technology, Inc.) and rabbit anti-cleaved caspase-3 antibody (1:1,000 dilution; cat. no. 9654; Cell Signaling Technology, Inc.) were used as primary antibodies, and were incubated at 4°C overnight. Membranes were incubated with horseradish peroxidase-conjugated goat anti-rabbit (1:10,000 dilution; cat. no. CW0234S; Beijing ComWin Biotech Co., Ltd.) and anti-mouse (1:10,000 dilution; cat. no. CW0221S; Beijing ComWin Biotech Co., Ltd.) immunoglobulin G secondary antibodies at 37°C for 1 h. The protein bands were determined by chemiluminescence (EMD Millipore). Densitometric analysis was performed using ImageJ version 1.8.0 (National Institutes of Health).

Cell viability. A549 cells were seeded in 96-well plates and incubated for 48 h following transfection. Subsequently, Cell Counting kit-8 (CCK-8, Dojindo Molecular Technologies, Inc.) was used for the examination of cell viability at 0, 12, 24 and 48 h of incubation. The number of cells was assessed with FLUOstar OPTIMA (BMG Labtech GmbH) at an absorbance wavelength of 450 nm.

Cell apoptosis. At 72 h after cell transfection, flow cytometry with Annexin V-fluorescein isothiocyanate (FITC)/propidium iodide (PI) was used for determination of cell apoptosis in the different groups. A549 cells were washed, trypsinized and resuspended in the staining solution provided in the Annexin V-FITC Apoptosis Detection kit (Invitrogen; Thermo Fisher Scientific, Inc.) according to the manufacturer's protocol. After 1 h of incubation of the cells with Annexin V-FITC antibody at 37°C, apoptosis was determined using a flow cytometer (BD Biosciences). The apoptotic cells presented with a positive Annexin V-FITC signal and a negative PI signal. The cell number at each phase was determined by FlowJo software version 7.6.3 (FlowJo LLC).

Dual-luciferase reporter assay. MAP4K3 was predicted to be a gene target for miR-98-5p by bioinformatics analysis using TargetScan release 7.1 (http://www.targetscan.org/vert_71). PCR was performed using the following thermocycling conditions: 94°C for 2 min, followed by 35 cycles of 94°C for 2 sec, 60°C for 60 sec and 72°C for 1 min with the following primers: MAP4K3 3'UTR forward, 5'-GGTACCAAAATAATTTAGTTACT-3' and reverse, 5'-CTCGAGTGAGGTAGTAAGT-3' and Platinum™ II Green PCR buffer (Thermo Fisher Scientific, Inc.). The PCR products were amplified using cDNA from 293T cells and fused to the firefly luciferase gene of the pGL3-control plasmid (Promega Corporation) with the restriction enzyme sites of *KpnI* and *XhoI*. Two site mutations were introduced to WT-MAP4K3-3'-UTR to construct the mutant (Mut) MAP4K3-3'-UTR by a Quick Site-directed

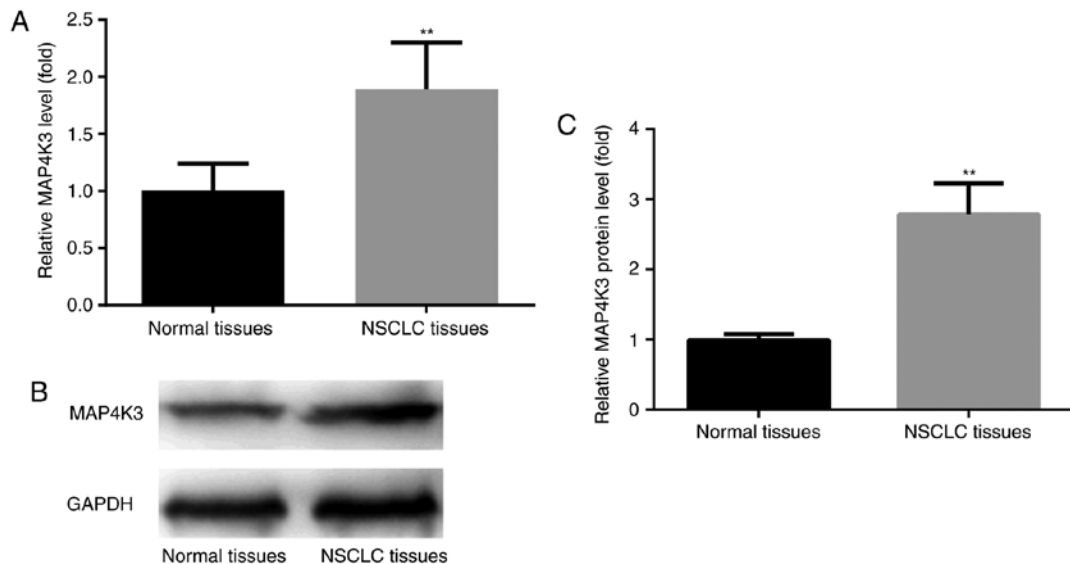


Figure 1. MAP4K3 expression is increased in tumor tissue from patients with NSCLC compared to adjacent normal tissue. There was a significant increase in MAP4K3 (A) mRNA and (B) protein levels in NSCLC tumor tissues compared with the adjacent normal tissues. (C) Quantification of protein levels. **P<0.01 vs. normal tissues. MAP4K3, mitogen-activated protein kinase kinase kinase kinase 3; NSCLC, non-small cell lung cancer.

mutation kit (Agilent Technologies, Inc.). The 293T cells were co-transfected with pGL3 constructions including 200 ng pGL3-WT-MAP4K3 and 200 ng pGL3-Mut-MAP4K3, 10 nM miR-NC or 10 nM miR-98-5p mimic and 26 ng pRL-TK in 24-well plates using Lipofectamine® 2000 (Invitrogen; Thermo Fisher Scientific, Inc.). At 24 h of transfection, luciferase activity (firefly and *Renilla*) was determined using the dual-luciferase reporter assay system (Promega Corporation).

Statistical analysis. Statistical analyses were performed using SPSS 13 software (SPSS, Inc.). Differences between two groups and among multiple groups were analyzed by Student's t-test and one-way analysis of variance followed by Newman-Keuls test, respectively. Results were presented as the mean ± standard deviation. P<0.05 was considered to indicate a statistically significant difference.

Results

MAP4K3 expression level is increased in NSCLC tumor tissues. To examine the expression level of MAP4K3, tumor tissues and their adjacent normal tissues from 90 NSCLC cases were analyzed using RT-qPCR and western blotting. The results revealed a significant increase in MAP4K3 mRNA levels in NSCLC tumor tissues compared with the adjacent normal tissues (Fig. 1A). The western blot results revealed that, compared with the adjacent normal tissues, MAP4K3 protein level was increased in NSCLC tumor tissues (Fig. 1B and C). These results were consistent with a previous report which showed that higher expression of MAP4K3 was associated with increased recurrence risk for lung cancer patients (14).

MAP4K3 is a target for miR-98-5p. MAP4K3 was predicted to be a gene target for miR-98-5p by bioinformatics analysis using TargetScan, and the binding sequences between positions 1,056-1,063 of the MAP4K3 3'-UTR and miR-98-5p are represented in Fig. 2A. In addition, other miRNAs were predicted

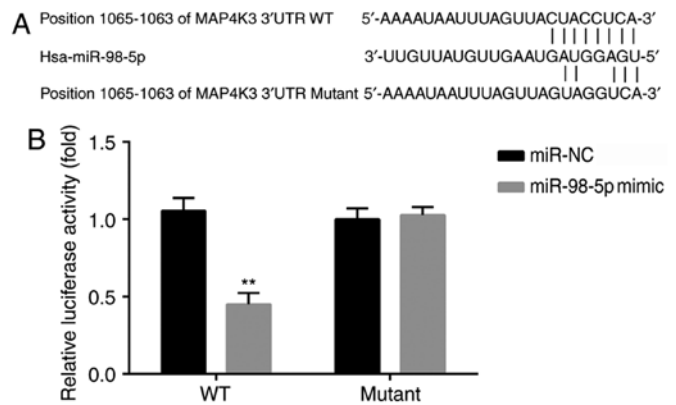


Figure 2. MAP4K3 is a target for miR-98-5p. (A) Binding sequence between positions 1,056-1,063 of the MAP4K3 3'-UTR and miR-98-5p sequence. (B) Dual luciferase reporter assay results indicating that 3'-UTR of MAP4K3 mRNA is a target of miR-98-5p. **P<0.01 vs. miR-NC. MAP4K3, mitogen-activated protein kinase kinase kinase kinase 3; miR, microRNA; UTR, untranslated region; NC, negative control; WT, wild-type.

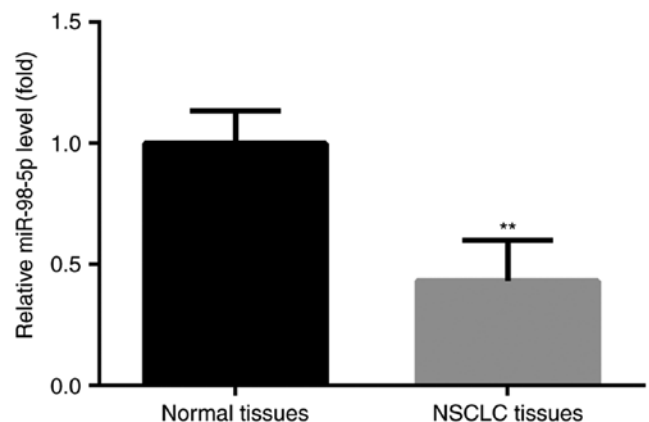


Figure 3. miR-98-5p expression is decreased in NSCLC tumor tissues. There was a significant decrease in miR-98-5p in NSCLC tumor tissue compared with the adjacent normal tissue. **P<0.01 vs. normal tissues. miR, microRNA; NSCLC, non-small cell lung cancer.

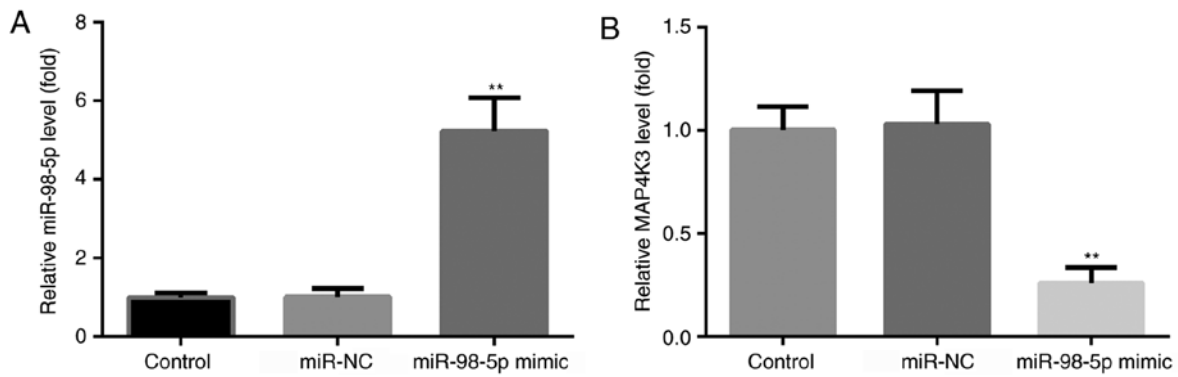


Figure 4. miR-98-5p mimic increases miR-98-5p expression and decreases MAP4K3 expression. (A) miR-98-5p expression and (B) MAP4K3 expression in A549 cells transfected with miR-98-5p mimic and control groups. ** $P < 0.01$ vs. miR-NC. miR, microRNA; MAP4K3, mitogen-activated protein kinase kinase 3; NC, negative control.

to target MAP4K3 based on the analysis by TargetScan. For instance, through literature review, let-7c was identified to be a regulator of MAP4K3 (19). As miR-98-5p is a member of the let-7 family, this miRNA was selected for investigation in the current study (13).

The 3'-UTR of MAP4K3 mRNA was verified to be a target for miR-98-5p by dual-luciferase reporter analysis. The relative luciferase activity in the cells transfected with wild type (WT) MAP4K3 3'-UTR and miR-98-5p mimic was significantly decreased compared with that observed in cells transfected with WT MAP4K3 3'-UTR and miR-NC. There was no significant difference in relative luciferase activity between cells transfected with mutant MAP4K3 3'-UTR and miR-98-5p mimic and cells transfected with mutant MAP4K3 3'-UTR and miR-NC (Fig. 2B).

miR-98-5p expression is decreased in NSCLC tumor tissues. The expression levels of miR-98-5p was determined in tumor tissues and adjacent normal tissues from 90 patients with NSCLC. The results revealed a significant decrease in miR-98-5p in NSCLC tumor tissues compared with the adjacent normal tissues (Fig. 3).

miR-98-5p overexpression increases miR-98-5p and decreases MAP4K3 levels. To examine the effects of miR-98-5p mimic on the expression changes of miR-98-5p and MAP4K3 in A549 cells, RT-qPCR was used. Compared with the control and miR-NC groups, an increase in miR-98-5p (Fig. 4A) and a decrease in MAP4K3 (Fig. 4B) levels were observed in the miR-98-5p mimic group.

miR-98-5p overexpression reduces cell viability. The effects of miR-98-5p on cell viability in NSCLC A549 cells were determined by CCK-8 assay. The growth curves demonstrated the effects of miR-98-5p on NSCLC cell viability. At 48 h of incubation following cell transfection, a significant decrease in cell viability was observed in the miR-98-5p mimic group compared with the control and miR-NC groups, whereas no significant differences were present at 0, 12 or 24 h of incubation (Fig. 5).

miR-98-5p overexpression induces cell apoptosis. The effects of miR-98-5p on cell apoptosis in the NSCLC cell line A549 were determined by flow cytometry. The results demonstrated

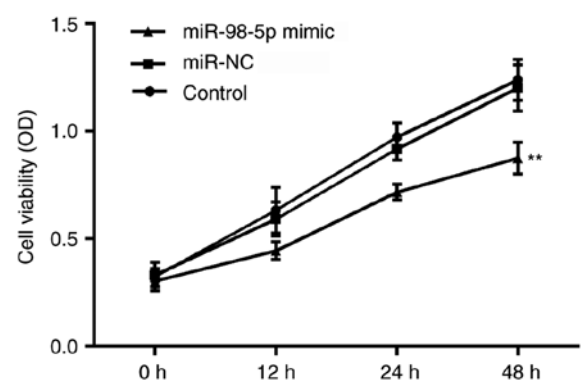


Figure 5. miR-98-5p mimic reduces cell viability. Compared with the control and miR-NC groups, there was a significant decrease in cell viability in the miR-98-5p mimic group. ** $P < 0.01$ vs. miR-NC. miR, microRNA; NC, negative control; OD, optical density.

that, compared with the control and miR-NC groups, there was a significant increase in cell apoptosis in the miR-98-5p mimic group (Fig. 6A and B).

miR-98-5p regulates MAP4K3 expression and the mTOR signaling pathway. To further examine the association between miR-98-5p and MAP4K3, as well as the potential regulatory mechanisms of miR-98-5p in the mTOR signaling pathway, the protein levels of associated molecules were determined by western blotting. As presented in Fig. 7A and B, the expression levels of MAP4K3 and p-mTOR were decreased, cleaved caspase-3 expression was increased, and the expression of mTOR was not significantly changed upon transfection with miR-98-5p mimic compared to control and miR-NC groups.

Discussion

Patients with NSCLC exhibit a median 5-year survival rate ranging from 26% (stage IIIA) to 51% (stage IA), which is lower than that of other types of cancer, including breast and prostate cancer (21). Despite the uncertain efficacy of chemotherapy, the most frequently used therapeutic method for the treatment of early-stage NSCLC is complete surgical resection alongside cisplatin-based chemotherapy (22). The results of the present study indicate that miR-98-5p, which was significantly

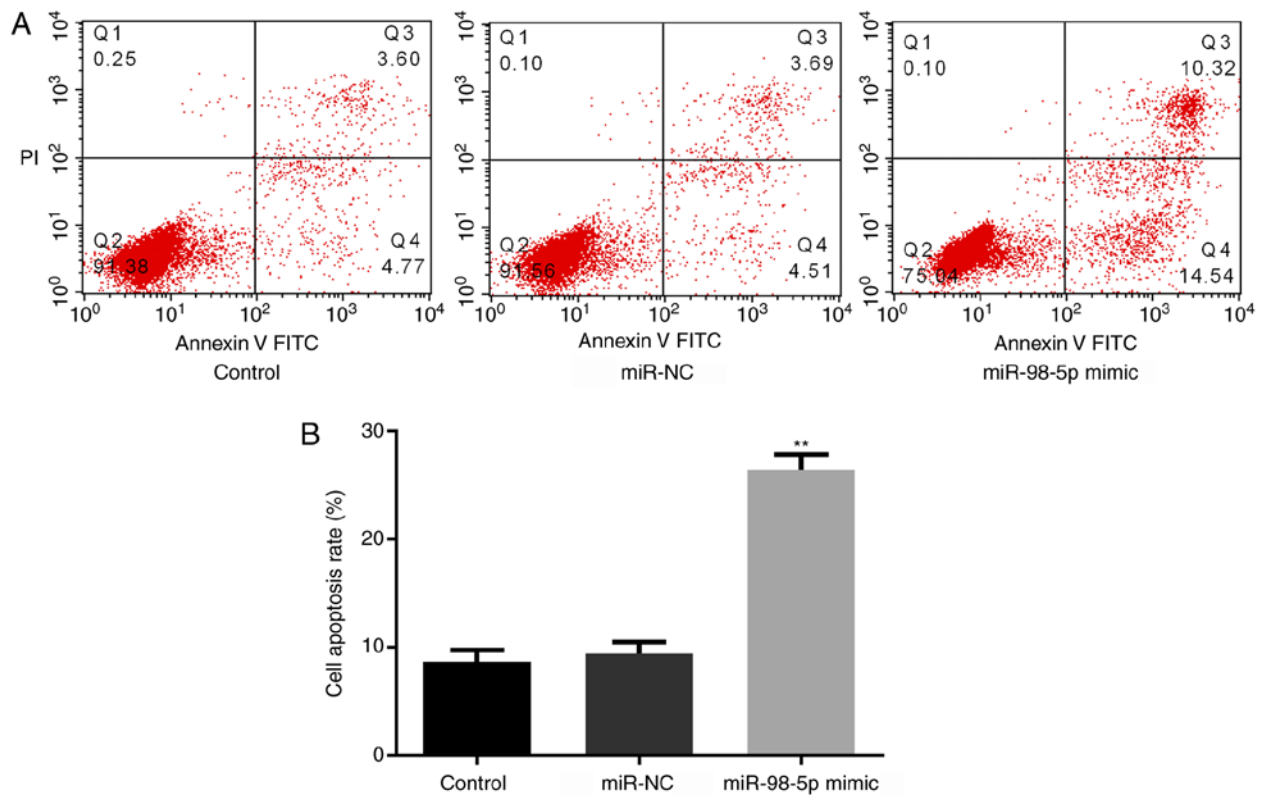


Figure 6. miR-98-5p mimic induces cell apoptosis. (A) Flow cytometry dot plots and (B) quantification of cell apoptosis in A549 cells transfected with miR-98-5p mimic and control groups. **P<0.01 vs. miR-NC. miR, microRNA; NC, negative control; PI, propidium iodide; FITC, fluorescein isothiocyanate.

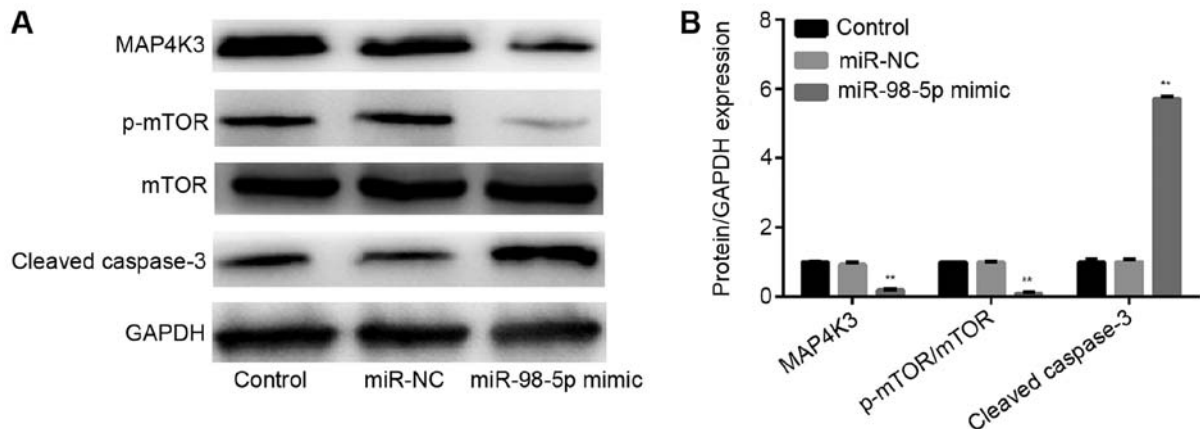


Figure 7. miR-98-5p regulates MAP4K3 expression and the activation of mTOR signaling pathway. (A) Western blot images and (B) quantification of protein expression showing that expression of MAP4K3 and p-mTOR was decreased, and cleaved caspase-3 was increased upon transfection with miR-98-5p mimic, while mTOR protein levels were not significantly changed. **P<0.01 vs. miR-NC. miR, microRNA; NC, negative control; MAP4K3, mitogen-activated protein kinase kinase kinase 3; mTOR, mammalian target of rapamycin; p-mTOR, phosphorylated mTOR.

decreased in NSCLC tumor tissues, could target MAP4K3 and inhibit the activation of the mTOR signaling pathway. These findings support an apical role for miR-98-5p/MAP4K3 in intracellular signal transduction cascades in NSCLC.

MAP4K3 is a protein kinase of the Ste20 family that is activated by ultraviolet radiation and the proinflammatory cytokine tumor necrosis factor- α (6). The present study demonstrated that MAP4K3, a target gene of miR-98-5p, was overexpressed in NSCLC tissues, while miR-98-5p was found to be downregulated. These findings indicate that miR-98-5p and MAP4K3 may serve roles in the progression of NSCLC.

The ability of tumor cells to increase cell number is determined by the cell proliferation rate and the extent of cell removal through apoptosis (23). Acquired resistance to apoptosis may be a hallmark of all cancer types (23). The present study investigated the effects of miR-98-5p on proliferation and apoptosis in A549 cells. It was observed that overexpression of miR-98-5p significantly inhibited cell proliferation and promoted apoptosis. These findings suggest a potential function of miR-98-5p as a therapeutic target for NSCLC. Previous studies have revealed that miRNA levels in tumors are variable, even among commercial cell lines, suggesting that further research is required to

determine the potential association between miRNA changes and clinical diagnostics or therapeutic treatments (24,25).

mTOR signaling is deregulated in multiple diseases including cancer (26). The present study revealed that miR-98-5p could significantly inhibit the activation of mTOR. This phenomenon indicated that miR-98-5p was able to regulate MAP4K3 expression and affect NSCLC cell activities via the mTOR signaling pathway.

However, the present study had limitations, as it was not directly demonstrated that altered MAP4K3 expression impacted proliferation and apoptosis of lung cancer cells. Future studies will investigate MAP4K3 overexpression in NSCLC cells and the interaction of MAP4K3 and miR-98-5p.

Acknowledgements

Not applicable.

Funding

No funding was received.

Availability of data and materials

The datasets used and/or analyzed during the current study are available from the corresponding author on reasonable request.

Authors' contributions

ZW, ZH, LZ, SZ performed the experiments and analyzed the data. BW conceived the study, analyzed the data and prepared the manuscript. All the authors read and approved the final version of manuscript for publication.

Ethics approval and consent to participate

The present study was approved by the Ethics Committee of General Hospital of Xuzhou Mining Group, The Second Affiliated Hospital of Xuzhou Medical University (Xuzhou, China). All patients or their families provided written informed consent prior to the start of the research.

Patient consent for publication

Not applicable.

Competing of interests

The authors declare that they have no competing interests.

References

- Dent AG, Suttedja TG and Zimmerman PV: Exhaled breath analysis for lung cancer. *J Thorac Dis* 5: S540-S550, 2013.
- Siegel R, Naishadham D and Jemal A: Cancer statistics, 2013. *CA Cancer J Clin* 63: 11-30, 2013.
- World Health Organization Classification of Tumors: Pathology and Genetics of Tumours of the Lung, Pleura, Thymus and Heart. William D. Travis WD, Elisabeth Brambilla E, Konrad Müller-Hermelink H and Harris CC (eds). IARC Press, Lyon, 2004.
- Wang T, Nelson RA, Bogardus A and Grannis FW Jr: Five-year lung cancer survival: Which advanced stage nonsmall cell lung cancer patients attain long-term survival? *Cancer* 116: 1518-1525, 2010.
- Hu MC, Qiu WR, Wang X, Meyer CF and Tan TH: Human HPK1, a novel human hematopoietic progenitor kinase that activates the JNK/SAPK kinase cascade. *Genes Dev* 10: 2251-2264, 1996.
- Diener K, Wang XS, Chen C, Meyer CF, Keesler G, Zukowski M, Tan TH and Yao Z: Activation of the c-Jun N-terminal kinase pathway by a novel protein kinase related to human germinal center kinase. *Proc Natl Acad Sci USA* 94: 9687-9692, 1997.
- Chuang HC, Sheu WH, Lin YT, Tsai CY, Yang CY, Cheng YJ, Huang PY, Li JP, Chiu LL, Wang X, *et al*: HGK/MAP4K4 deficiency induces TRAF2 stabilization and Th17 differentiation leading to insulin resistance. *Nat Commun* 5: 4602, 2014.
- Chen YR and Tan TH: Mammalian c-Jun N-terminal kinase pathway and STE20-related kinases. *Gene Ther Mol Biol* 4: 83-98, 1999.
- Chen YR and Tan TH: The c-Jun N-terminal kinase pathway and apoptotic signaling (review). *Int J Oncol* 16: 651-662, 2000.
- MacCorkle RA and Tan TH: Mitogen-activated protein kinases in cell-cycle control. *Cell Biochem Biophys* 43: 451-461, 2005.
- Lam D, Dickens D, Reid EB, Loh SH, Moiso N and Martins LM: MAP4K3 modulates cell death via the post-transcriptional regulation of BH3-only proteins. *Proc Natl Acad Sci USA* 106: 11978-11983, 2009.
- Liu L, Lu L, Zheng A, Xie J, Xue Q, Wang F, Wang X, Zhou H, Tong X, Li Y, *et al*: miR-199a-5p and let-7c cooperatively inhibit migration and invasion by targeting MAP4K3 in hepatocellular carcinoma. *Oncotarget* 8: 13666-13677, 2017.
- Zhao B, Han H, Chen J, Zhang Z, Li S, Fang F, Zheng Q, Ma Y, Zhang J, Wu N and Yang Y: MicroRNA let-7c inhibits migration and invasion of human non-small cell lung cancer by targeting ITGB3 and MAP4K3. *Cancer Lett* 342: 43-51, 2014.
- Hsu CP, Chuang HC, Lee MC, Tsou HH, Lee LW, Li JP and Tan TH: GLK/MAP4K3 overexpression associates with recurrence risk for non-small cell lung cancer. *Oncotarget* 7: 41748-41757, 2016.
- Guo H, Ingolia NT, Weissman JS and Bartel DP: Mammalian microRNAs predominantly act to decrease target mRNA levels. *Nature* 466: 835-840, 2010.
- Markou A, Tsaroucha EG, Kaklamanis L, Fotinou M, Georgoulas V and Lianidou ES: Prognostic value of mature microRNA-21 and microRNA-205 overexpression in non-small cell lung cancer by quantitative real-time RT-PCR. *Clin Chem* 54: 1696-1704, 2008.
- Bueno MJ, Pérez de Castro I and Malumbres M: Control of cell proliferation pathways by microRNAs. *Cell Cycle* 7: 3143-3148, 2008.
- Jovanovic M and Hengartner MO: miRNAs and apoptosis: RNAs to die for. *Oncogene* 25: 6176-6187, 2006.
- Wang Y, Bao W, Liu Y, Wang S, Xu S, Li X, Li Y and Wu S: miR-98-5p contributes to cisplatin resistance in epithelial ovarian cancer by suppressing miR-152 biogenesis via targeting Dicer1. *Cell Death Dis* 9: 447, 2018.
- Livak KJ and Schmittgen TD: Analysis of relative gene expression data using realtime quantitative PCR and the 2(Delta Delta C(T)) method. *Methods* 25: 402-408, 2001.
- Chuang JC, Neal JW, Niu XM and Wakelee HA: Adjuvant therapy for EGFR mutant and ALK positive NSCLC: Current data and future prospects. *Lung Cancer* 90: 17, 2015.
- NSCLC Metaanalyses Collaborative Group, Arriagada R, Auperin A, Burdett S, Higgins JP, Johnson DH, Le Chevalier T, Le Pechoux C, Parmar MK, Pignon JP, *et al*: Adjuvant chemotherapy, with or without postoperative radiotherapy, in operable nonsmallcell lung cancer: Two metaanalyses of individual patient data. *Lancet* 375: 1267-1277, 2010.
- Hanahan D and Weinberg RA: The hallmarks of cancer. *Cell* 100: 57-70, 2000.
- Dumache R, Rogobete AF, Andreescu N and Puiu M: Genetic and epigenetic biomarkers of molecular alterations in oral carcinogenesis. *Clin Lab* 61: 1373-1381, 2015.
- Zahrn F, Ghalwash D, Shaker O, Al-Johani K and Scully C: Salivary microRNAs in oral cancer. *Oral Dis* 21: 739-747, 2015.
- Soulard A and Hall MN: SnapShot: mTOR signaling. *Cell* 129: 434, 2007.